Fuel 101 (2012) 197–204

Contents lists available at ScienceDirect

Fuel

journal homepage: www.elsevier.com/locate/fuel

Pyrrhotite deposition through thermal projection to simulate iron sulphide slagging in oxyfuel combustion

M.C. Mayoral *, J.M. Andrés, M.T. Izquierdo, B. Rubio

Instituto de Carboquímica, CSIC, Zaragoza, Spain

ARTICLE INFO

Article history:
Received 1 October 2010
Received in revised form 28 June 2011
Accepted 30 June 2011
Available online 21 July 2011

Keywords:
Slagging
Oxyfuel
Corrosion
Pyrrhotite

ABSTRACT

Oxyfuel combustion is envisaged as one of the main options for near future CO_2 reduction in conventional power production. There are many aspects of oxy-combustion still at the research stage. One of those is the issue of boiler materials resistance to corrosion due to solid deposits formed as a consequence of slagging in CO_2 rich flue gases. The novel approach to the issue is the simulation of realistic slagging by pyrite (FeS_2) projection through an oxyacetylene spray gun, flying along a controlled flame and impacting onto metallic surfaces of selected composition for fireside waterwall construction (F22, P91, 409, 347, 304H, and 800HT). Metallic surface temperatures were kept at 400, 500, 600 or 700 °C, and after deposition, metallic coupons were aged for long periods (150 and 1500 h) at the selected conditions (O_2/N_2, CO_2/N_2). The characterisation of deposits was performed with XRD, SEM-EDX and carburisation tests.

The first finding is that the oxidation progression is different when partially transformed pyrite covers metallic surfaces. In that case, no iron oxide (Fe_2O_3) scale is generated, only the chromium oxide (Cr_3O_4) grows between the steel and the deposit as a response to oxidation. There is a clear presence of chromium sulphides in competition with the chromium oxide. On the other hand, comparison of scales in CO_2 vs. air indicates the same chemical composition but different morphology; in air combustion, corrosion layers are thicker and cracked. These results can improve the prediction of operational problems in coal oxy-fuel combustion.

1. Introduction

Oxy-fuel coal combustion is envisaged as a promising technology for near future CO_2 reduction from conventional fuel power plants. There is significant public and private effort in the development of demonstration plants and calculations of final economic feasibility of carbon emission reduction using oxy-fuel combustion. Ash related problems are still a matter of concern, and are recognised as a major source of uncertainty in the technology [1]. In fact, slagging, fouling, corrosion and fuel blending are still coal quality related issues to be addressed and solved in commercial power plants [2]. Among the mineral constituents of coal, pyrite (FeS_2) is considered the main cause of slagging on fireside heat transfer surfaces, leading to operational problems and materials failure. The background of the problem is well-known: pyrite plays a mayor role in slagging due to the formation of low melting FeS–FeO intermediates (eutectic point at 940 °C) and the fluxing effect of FeO in aluminosilicates [3,4]. Early studies on pyrrhotite ($Fe_{1-x}S$) from coal pyrite [5,6] defined a multiphase thermochemistry model still in use, whereas knowledge of the kinetics is less precise [7]. For this reason, recent studies on iron transformations in coal combustion include drop tube reactors for realistic conditions and instrumental techniques for characterisation [8–10]. The concern in pyrite transformation is renewed for the case of CO_2 recirculation in oxyfuel combustion [11,12]. In the present work, pyrite evolution has been studied using simultaneous differential scanning calorimetry–thermogravimetry (DSC–TGA), which proved very successful in describing deposition and fluxing phenomena in slagging conditions [13]. These results are compared to real scale deposits: the new approach in this work is the use of a flame spraying gun, where pyrite particles are dispersed inside a controlled flame at fast heating rates. Solid particles can attain 1800 °C in milliseconds, reaching the melting point, thus resembling realistic conditions inside burners. Moreover, due to the fast particle velocities in projection guns, molten droplets splat onto projection surfaces ensuring a high degree of contact between deposit and metallic surface. In this way deposits are obtained at controlled surface temperatures, and chemical composition is characterised by XRD and SEM as a function of gas temperature and gas composition, from air to complete CO_2 recirculation as in oxyfuel combustion. Examples of experimental evaluation of the fireside corrosion resistance can be found in the literature for

* Corresponding author. Address: Instituto de Carboquímica, CSIC, Miguel Luesma n. 4, 50018 Zaragoza, Spain.
E-mail address: mayoral@icb.csic.es (M.C. Mayoral).

0016-2361/$ - see front matter © 2011 Elsevier Ltd. All rights reserved.
doi:10.1016/j.fuel.2011.06.063

oxycombustion [14,15], although the present work is the first one focused in iron sulphide deposits impact in waterwall corrosion.

2. Experimental

Natural pyrite from coal rejects was sieved between 100 μm > dp > 30 μm and stored under an inert atmosphere. Metallic materials were selected based on their chromium content (purchased from Metal Samples Company Inc.) with complete compositions shown in Table 1.

The thermobalance TA Inst. Q600 allows simultaneous thermogravimetry and calorimetry. Samples were laid onto the tared Pt pans and heat treatments consisted of heating ramps of 50 °C min^{-1} to the desired temperature. A constant flow of 100 ml min^{-1} was maintained for all the purge gas studied: N_2, CO_2, and their mixtures.

The phase composition of the iron species was investigated applying X-ray diffraction using a Siemens D500 diffractometer set to select Cu Kα radiation. The diffraction angle scanned was 20–70° 2θ using a step size of 0.05° 2θ.

The sulphur content in samples was determined in a Carlo-Erba-1108 elemental analyser.

For solids projection, a 5PII Sulzer Metco gun was selected, operated with hydrogen as fuel. The system comprised two Witt MM-Flex gas mixers with a proportional mixing valve and variable flow settings. Stable flames were obtained with air or O_2/CO_2–N_2 mixtures. A specific software (Gaseq) was used to obtain the adiabatic flame temperature and final flue gas composition for each initial gas composition. Real temperature was measured with a type S thermocouple along flame prior to solids injection. Particle velocity was monitorised by the in-flight particle sensor Accuraspray [16].

Metallic coupons were placed along flame axial line at several fixed distances, so that the specific coupon temperature is ranging from 400 to 700 °C. Temperature was measured by a type K contact thermocouple in the reverse of the coupon. Once the selected temperature was reached, the gun was triggered and pyrite powder flowed along flame and impacted. Projection was maintained for two minutes to obtain a desired depth of deposit. Surface composition was analysed for each sample by X-ray diffraction.

After analysis, samples were exposed in a furnace for 150 h and 1500 h periods in a constant flow of 50 ml min^{-1} O_2/N_2 and CO_2/N_2, at 500 and 600 °C. Bare metallic coupons were aged at the same conditions as blank experiments to establish comparison with the projected metallic coupons. The composition of polished cross-section of samples was studied by means of scanning electron microscopy in a Hitachi S-3400N microscope equipped with a Si(Li) EDX detector Röntec XFlash.

3. Results

3.1. Thermogravimetry

The decomposition of pyrite with temperature was followed using simultaneous thermogravimetry and differential calorimetry. Weight changes along thermal treatment confirmed that the decomposition of pyrite to pyrrhotite occurs between 500 and 700 °C, as follows:

$$FeS_2 \rightarrow Fe_{1-x}S + 1/2S_2 \quad (1)$$

The extent and temperature range of decomposition was the same for CO_2 and N_2. Fig. 1 shows the evolution of enthalpy (in arbitrary units) with temperature, where the endothermic peaks of pyrite decomposition are clearly seen. As temperature increased, iron monosulphides reached their molten state, seen as endothermic peaks in Fig. 1. In differential calorimetry, the melting point is the graphic onset of the endotermic melting peak, and the enthalpy can be calculated from the peak area. Fig. 1 shows that melting points were different depending on the purge gas: pyrrhotite melted at 1080 °C in N_2, whereas the onset temperature of the first endothermic peak was 980 °C in CO_2. New thermobalance experiments were performed, stopping the heating ramp just after the decomposition peak and before the melting peaks. Final composition of samples was determined by XRD (Fig. 2a–c): pyrrhotite was the only species when heating in N_2, whereas in CO_2, there was magnetite (Fe_3O_4) present in the sample. It was proposed in the literature that CO_2 dissociates in CO and O_2 after heating to 500 °C, so transformation in CO_2 could involve partial oxidation to magnetite, in accordance with the following reaction path [12]:

$$FeS_2 + CO_2(g) \rightarrow Fe_3O_4 + Fe_2O_3 + COS(g) + SO_2(g) \quad (2)$$

Although further oxidation of magnetite to haematite (Fe_2O_3) is described in the equation, no traces of Fe_2O_3 were detected in the diffractograms.

A semi-quantitative analysis of the two main possible crystalline species (pyrrhotite and magnetite) was performed with the software package EVA 8.0 (Socabim Inc., Bruker AX Systems) by the Reference Intensity Ratios (RIR) method. Semi-quant XRD final composition is given in Table 2. It is worth mentioning that these compositions were in accordance with the weight changes registered in thermogravimetry due to the theoretical sulphur loss-oxygen gain. Sulphur content of samples was obtained by elemental analysis (Table 2). Provided that XRD detected only pyrrhotite

Table 1
Composition in weight percentage of the metallic materials selected.

wt%	Fe	Cr	Ni	Mo
F22	96.07	2.28	–	0.90
P91	88.86	8.78	0.12	0.97
409	87.61	11.2	0.19	–
347	69.60	17.45	9.43	0.32
304H	71.70	18.16	8.16	0.05
I800HT	45.69	19.88	31.29	–
I617	1.03	21.93	54.66	8.84
I690	8.98	28.8	61.20	–

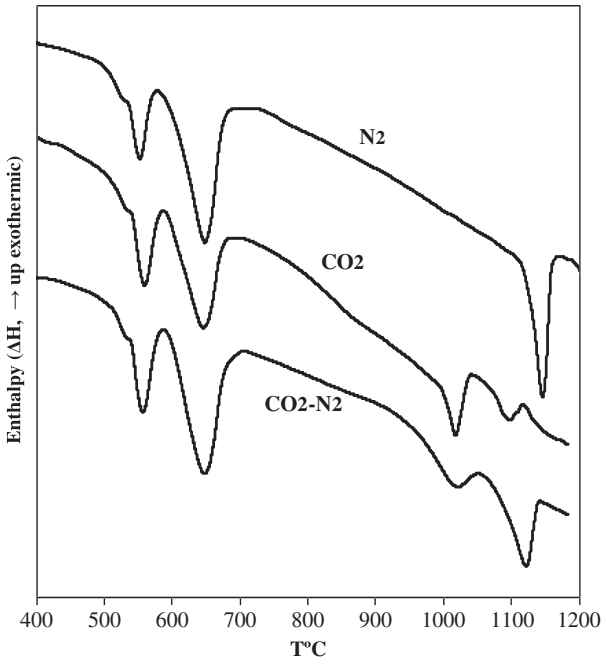

Fig. 1. Heat flow profiles in differential scanning calorimetry of natural pyrite in N_2, CO_2 and a mixture 50%CO_2–N_2 as purge gases. (a.u.): Arbitrary units.